Computers and Concrete, *Vol.15, No.4 (2015) 485-501*
DOI: http://dx.doi.org/10.12989/cac.2015.15.4.485

A meso-scale approach to modeling thermal cracking of concrete induced by water-cooling pipes

Chao Zhang[1,2a], Wei Zhou[*1], Gang Ma[1b], Chao Hu[1c] and Shaolin Li[1d]

[1]*State Key Laboratory of Water Resources and Hydropower Engineering Science*, *Wuhan University*, *430072*, *Wuhan*, *Hubei Province*, *People's Republic of China*
[2]*Changjiang Survey Planning Design & Research Company Limited*, *430010*, *Wuhan*, *Hubei Province* *People's Republic of China*

(*Received August 29, 2014, Revised January 12, 2015, Accepted January 30, 2015*)

Abstract. Cooling by the flow of water through an embedded cooling pipe has become a common and effective artificial thermal control measure for massive concrete structures. However, an extreme thermal gradient induces significant thermal stress, resulting in thermal cracking. Using a mesoscopic finite-element (FE) mesh, three-phase composites of concrete namely aggregate, mortar matrix and interfacial transition zone (ITZ) are modeled. An equivalent probabilistic model is presented for failure study of concrete by assuming that the material properties conform to the Weibull distribution law. Meanwhile, the correlation coefficient introduced by the statistical method is incorporated into the Weibull distribution formula. Subsequently, a series of numerical analyses are used for investigating the influence of the correlation coefficient on tensile strength and the failure process of concrete based on the equivalent probabilistic model. Finally, as an engineering application, damage and failure behavior of concrete cracks induced by a water-cooling pipe are analyzed in-depth by the presented model. Results show that the random distribution of concrete mechanical parameters and the temperature gradient near water-cooling pipe have a significant influence on the pattern and failure progress of temperature-induced micro-cracking in concrete.

Keywords: concrete; mesoscopic simulation; equivalent probabilistic model; thermal cracking; micro-cracking

1. Introduction

Controlling temperature-induced cracking is one of the main concerns in the design and construction of mass concrete. Since the construction of Hoover Dam, cooling by the flow of water through an embedded cooling pipe has become a common and effective artificial temperature-control measure in the construction of massive concrete structures. However, great temperature stress can be caused by large temperature changes and gradients, especially mass

∗Corresponding author, Ph.D. Professor, E-mail: zw_mxx@163.com
[a]Ph.D. Student, E-mail: gonopo@whu.edu.cn
[b]Ph.D. Lecturer, E-mail: magang630@163.com
[c]Ph.D. Student, E-mail: huchao1214@163.com
[d]Ph.D. Student, E-mail: shaolin@whu.edu.cn

http://www.techno-press.org/?journal=cac&subpage=8 ISSN: 1598-8198 (Print), 1598-818X (Online)

concrete in which the volume fraction of coarse aggregate is generally up to 60-70% used. (Amin. *et al*. 2009). In fact, concrete is a typical complex heterogeneous material, which is made of an aggregate with nonhydrated granules and cement with numerous capillary grains. Some failure mechanisms, such as the aggregate inter-locking and softening behaviors due to micro-cracking, actually occur at a finer scale. Since 1985, when three dimensions of macro, meso and micro were introduced to concrete material research by Wittmann, mesostructure-based modeling and random distributing techniques have been recognized as important research areas in engineering and materials science (Wittmann *et al*. 1985).

In the present mesoscopic approach to modeling the fracture process and evaluating the macroscopic response of concrete, concrete is always treated as a three-phase composite, aggregates, mortar matrix and ITZs between them. Strength and fracture behavior of concrete influenced by aggregate shape and packing forms (Yasar *et al*. 2004, Elices and Rocco 2008, 2009, He *et al*. 2011), loading concepts (Yan and Lin 2006) and size effects (Almusallam *et al*. 2004, Tang *et al*. 2011) have been extensively covered by both experimental and numerical studies. Numerical fracture models such as continuum models (Peerlings 1999, Jirásek and Marfia 2005), discontinuous models based on the extended FE method (Wells and Sluys 2001), discrete models (Wanne *et al*. 2007, Azevedo *et al*. 2010) and lattice models (Grassl *et al*. 2010, Qian 2011) indicate that the fracture process zone is governed by both statistics and mechanics. Hence, instead of simulating the multiphase components of concrete, an equivalent approach for studying the heterogeneity of concrete by introducing the Weibull probabilistic distribution for describing heterogeneities of mechanical and statistical properties of concrete (Tang and Zhu 2003, Tang X., *et al*. 2011), gives a good estimate of the weakening zone and successfully characterizes the localization of the fractures. Although many achievements have been made in the analysis of material mechanical properties by the mesoscopic approach in recent years, the approach still lacks an effective way to simulate concrete temperature-induced cracking, and to explore the mechanism, especially for the complexity of concrete temperature fields, which are greatly affected by water-cooling pipes, such as in concrete dams.

In this paper, a 2D meso-scale concrete model is divided into three phases, aggregate, mortar matrix and ITZs, in which random convex polygon aggregates with actual gradient and size are modelled. Subsequently, an equivalent probabilistic model improved by introducing a statistical correlation coefficient between elastic modulus and tensile strength into the Weibull distribution law is presented by using a mesoscopic FE mesh. Moreover, in contrast to the laboratory test approach of other researchers, mechanical parameters of the equivalent probabilistic model using the statistical method are verified by a series of numerical experiments. In the final part, the description of temperature in concrete cooled by water pipes is precisely simulated, and temperature cracks' initiation, propagation and coalescence in concrete induced by cooling water with mesoscopic heterogeneous mechanical parameters are extensively studied by contrast with macroscopic homogeneous mechanical parameters. The propagation pattern and process of concrete temperature cracks with cooling pipes are described in detail. The meso-scale approach may be employed to provide guidance on choosing a reasonable temperature difference between concrete and cooling water in mass concrete engineering.

2. Meso-scale model for concrete

Aggregate takes up most of the volume of concrete, and it also strongly governs its mechanical

properties. In previous numerical analyses, aggregates were conventionally assumed to be circular or spherical (Zhou and Hao 2008). However, aggregates in concrete generally are produced by the crushing of large stones with outward-convex shape and various sizes. In this paper, circles with given diameter are generated by the Monte Carlo method, and then convex polygons satisfying the specified size are produced by connecting vertices which are randomly selected on the circle. As shown in Fig. 1, vertices of convex polygons on the circle are determined by the polar coordinates

$$\varphi_i = 2\pi[1+(2b_i-1)\delta]/n \tag{1}$$

in which φ_i is the angle corresponding to the center of edge i($1\le i\le$n); n($4\le$n≤ 8) is the number of polygon edges; b_i($0<b_i\le$n) is a random number; δ=0.65 is a constant.

The number and size distribution of aggregate are illustrated by Fuller's curve according to the Walraven grading function (Walraven *et al*. 1981).For a given type of aggregate, the take-and-place method (Wang and Kwan 1999) is used to determine the size and spatial position of the aggregates. As shown in Fig. 2, assuming a convex polygon aggregate is composed of n vertices numbered 1 to n, the corresponding coordinates are $(x_1,y_1),(x_2,y_2),\ldots,(x_n,y_n)$. The area surrounded by any node P(x, y) and two adjacent vertices i, i+1(i=1, 2…, n) can be calculated by Eq. (2).

$$S_i = \frac{1}{2}\begin{vmatrix} x & y & 1 \\ x_i & y_i & 1 \\ x_{i+1} & y_{i+1} & 1 \end{vmatrix} \tag{2}$$

If $S_i>0$(i=1,2,3,…,n-1), P is in the convex polygon; If $S_i=0$($i=k$, $k\in$(1, 2, …, n)) and $S_i=0$($i\neq k$, $i\in$(1,2,…,n)), P is on the edges of the convex polygon; otherwise, P is outside of the polygon.

For a given mesoscopic FE mesh, if all nodes of an element are located in the convex polygon, the element is identified as aggregate; if all nodes are located outside of the convex polygon, then the element is recognized as mortar; for the rest, the element is identified as ITZ. By the proposed method, the three-phase composite model of concrete can be divided, as shown in Fig. 3.

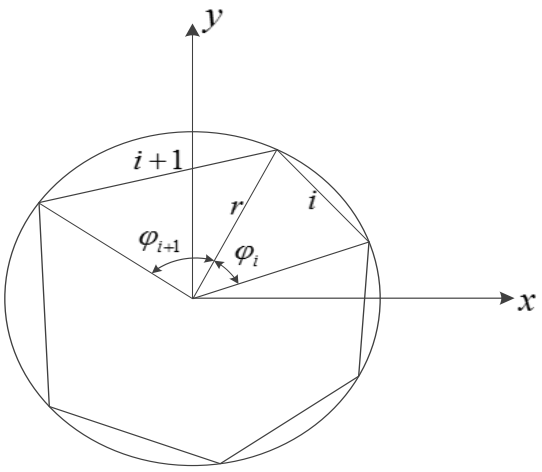

Fig. 1 Generation of convex polygons aggregate

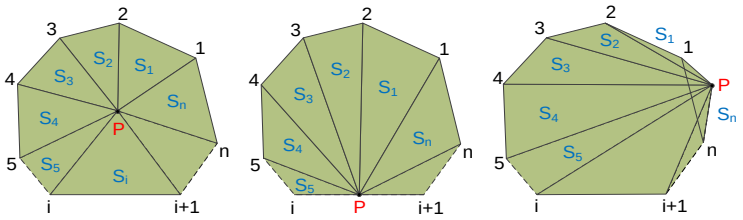

Fig. 2 Location relation of node and convex polygon

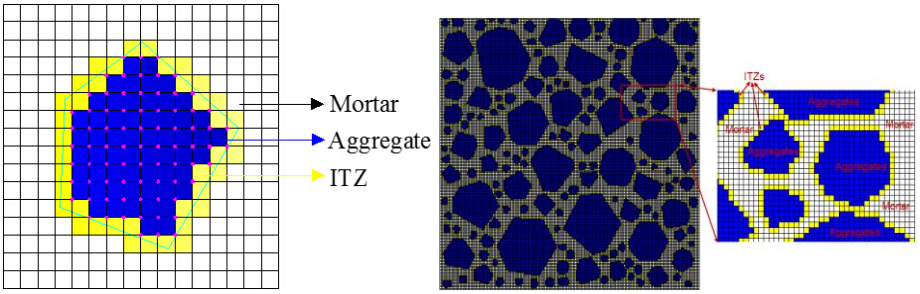

Fig. 3 Differentiation methods of three-phase in concrete mesoscopic model

3. Equivalent probabilistic model based on the improved weibull distribution law

To consider the influence of material heterogeneity on macroscopic mechanical behaviors of concrete, elastic modulus (E) and uniaxial tensile strength f_t of each element were assumed to conform to the Weibull distribution law, which can be illustrated as the following statistic density f(x) and distribution function F(x) (Van Mier *et al*. 2002):

$$f(x) = \frac{m}{u}\left(\frac{x}{u}\right)^{m-1} \exp\left[-\left(\frac{x}{u}\right)^{m}\right]$$
$$F(x) = 1 - \exp\left(-\left(\frac{x}{u}\right)^{m}\right) \tag{3}$$

where x was mechanical parameter obeying the Weibull distribution law (such as E or f_t); u was scale parameter corresponding to average value; m was the heterogeneity index, which defined the degree of material homogeneity (Tang and Zhu 2003). To reflect the relationship between E and f_t, the correlation coefficient ρ was introduced, which can be expressed by Eq. (4):

$$ran_1 = \sqrt{-2\log(r_1)}\cos(2\pi r_2)$$
$$ran_2 = ran_1\rho + \sqrt{-2\log(r_3)}\cos(2\pi r_4)\sqrt{1-\rho^2}$$
$$E = u_E(-In(ran_1))^{1/m_E} \tag{4}$$
$$f_t = u_{f_t}(-In(ran_2))^{1/m_{ft}}$$

in which r_1,r_2,r_3,r_4 were uniform random numbers between 0 and 1; u_E, m_E were the expected probability and heterogeneity index of E by the Weibull distribution; u_{f_t}, m_{f_t} were the expected probability and heterogeneity index of f_t by the Weibull distribution.

4. Damage evolution model

A simple bilinear damage model (Tang Xinwei *et al*. 2011) was applied for the description of the mechanical behavior of each concrete phase. Experimental studies showed that nonlinearity of the stress-strain relationship occurred because of continuous damage caused by micro crack initiation and propagation (Nooru-Mohamed 1992). The process was described by stiffness degradation, which can be expressed as Eq. (5) and Fig. 4.

$$\begin{aligned} \boldsymbol{\sigma} &= \boldsymbol{E}\boldsymbol{\varepsilon} \\ \boldsymbol{E} &= \boldsymbol{E_0}(1-D), (0 \le D \le 1) \end{aligned} \tag{5}$$

in which $\boldsymbol{E_0}$ and $\boldsymbol{E}$ were elastic modulus of undamaged and damaged material, respectively; D represented the damage variable, which was defined by:

$$D = \begin{cases} 0 & \varepsilon < \varepsilon_t \\ 1-(\dfrac{f_t + E_1\varepsilon_t}{E_\varepsilon} - \dfrac{E_1}{E_0}) & \varepsilon_t < \varepsilon < \varepsilon_m \\ 1-\dfrac{E_2}{E_0}(\dfrac{\varepsilon_f}{\varepsilon}-1) & \varepsilon_m < \varepsilon < \varepsilon_f \\ 1 & \varepsilon_f < \varepsilon \end{cases} \tag{6}$$

where f_t was tensile strength, f_m denoted residual strength at the turning point M, ε_t and ε_m were two principal tensile strains corresponding to f_t and f_m; ε_f was the ultimate tensile strain. Herein, elastic modulus of different periods can be expressed as $E_0=f_t/\varepsilon_t$, $E_1=(f_t-f_m)/(\varepsilon_t-\varepsilon_m)$, $E_2=f_m/(\varepsilon_t-\varepsilon_m)$; ξ, η were residual strength coefficient and ultimate strain coefficient of the element, respectively, which can be defined as $\xi=f_m/f_t=1/3$, $\eta=(\varepsilon_f-\varepsilon_t)/(\varepsilon_t-\varepsilon_m)=8$. The maximum tensile stress criterion was chosen as the strength criterion in this study. Only tensile cracking was considered, whereas a material point under pure compression was assumed as being linear elastic. Mesh sensitivity was an inherent problem of traditional local damage models, the reliability of the numerical simulation largely depended on mesh fineness. For avoiding mesh sensitivity, the fracture energy conservation principle was proposed by Bazant (Bazant *et al*. 1983), the damage softening stress-strain relation was adjusted based on mesoscopic element size and fracture energy. To solve this problem of the isotropic damage model in this study, energy regularization was applied, with ε_f defined by:

$$\varepsilon_f = \frac{\lambda}{l}(\varepsilon_f - \frac{\varepsilon_t}{2}) + \frac{\varepsilon_t}{2} \tag{7}$$

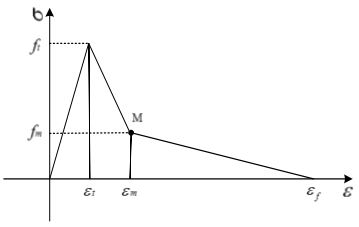

Fig. 4 Stress-strain relationship of the damage model

Herein, λ was defined as the width of the damage zone which controls the localization of deformation in the failure state, a simple approach was adopted that for plane element, the square root of the integration point volume was taken as the width of the localization band. l was a parameter related to the element size. This conventional method had been covered by other researchers before (He *et al*. 2011, Brekelmans *et al*. 1995).

5. Verification analysis

In this section, the uniaxial tensile test is chosen for validating the implementation of the proposed method. A series of analyses using different correlation coefficient factors has been performed to investigate its influence on the damage and failure response and the assessment of the material strength property. The specimen size is 200 mm × 200 mm. The plane stress assumption is made and the specimen is discretized into 1 mm × 1 mm FEs; accordingly, a total of 40,000 elements are meshed in the numerical model, including 24,053 aggregate elements, 11,456 mortar elements and 4,491 ITZ elements. Other information about the material properties of the three phases, dimensions, loading and boundary conditions is given in Tables 1 and 2 and Fig. 5. These values are in the range used for other meso-scale analyses (Grassl *et al*. 2010, Tang *et al*. 2008).

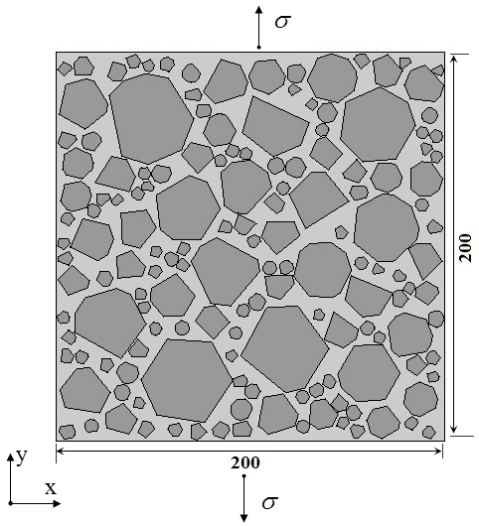

Fig. 5 Geometry and loading setup of the uniaxial tensile test

Table 1 Characteristic of aggregate in the numerical concrete model

Particle size（mm）		5-10	10-20	20-40
Ratio to total aggregate volume（%）		25	32	43
Total volume fraction (60%)	Volume（m^2）	0.034	0.052	0.066
	numbers	123	34	9

Table 2 Mechanical parameters for numerical uniaxial tensile test of concrete

Phase	E /GPa	f_t/MPa	ρ	m	μ
Aggregate	60	8.0	0.9	6	0.2
Mortar	38	3.5	0.9	3	0.2
ITZ	23	2.2	0.9	9	0.2

5.1 uniaxial tensile test

Twenty test samples with random meso-scale mechanical parameters are generated according to Table. 2. The modeling results of the stress-strain curves and damage and failure response are shown in Figs. 6 and 7. In addition, a comparison with the experimental stress-strain curve is made in Fig. 6 (Tang *et al*. 2008). Because of a different distribution of mechanical parameters of meso-scale elements in each sample, the stress-strain curves are therefore different. At earlier stages of analysis, stress-strain curves show a linear character because of linear elastic properties of materials. With continued loading, damage occurs mainly in the ITZs because of the low strength, and then distributed cracking occurs. Shortly after the stress peak (Fig. 6), many of these cracks connect with one another and cease to grow. Stress-strain curves of the uniaxial tensile test have a good agreement with the test by Tang, whose stress-strain curves are in the envelope of the 20 meso-scale numerical analyses. The maximum tensile strength of the 20 meso-scale numerical analyses is between 2.48-2.6 MPa.

The entire process of cracks' initiation, propagation and connection is exhibited, and elements with D>0.9 are shaded with a red point color (Fig. 7). Most of the cracks are located and extended in the ITZs and mortar matrix; cracks occur only rarely in aggregate. When cracks occur, the stress concentration region forms near the cracks, and new cracks readily appear together with the sustained loading. Cracks are usually impeded from extending to the aggregate because of its relatively high tensile strength. Finally, macro cracks form as a result of concatenation of the micro cracks, and the propagation direction of macro cracks is usually approximately perpendicular to the loading direction. In addition, many micro cracks randomly grow at different specimen positions, which indicates that the internal defects in the concrete have a great effect on its strength and failure pattern.

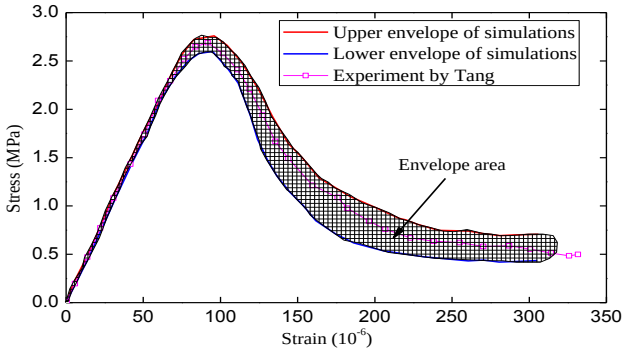

Fig. 6 Stress-strain curves under uniaxial tension

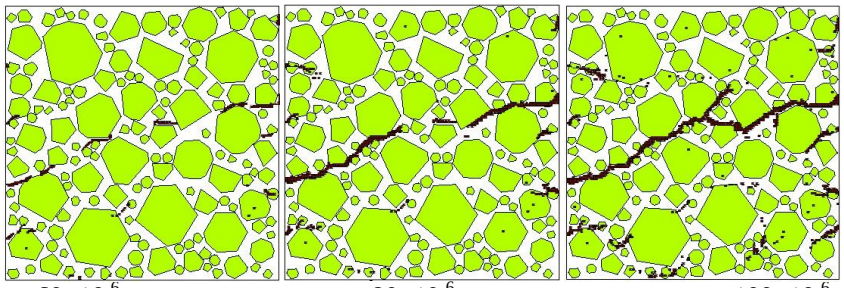

Fig. 7 Failure pattern of concrete specimens at different load steps

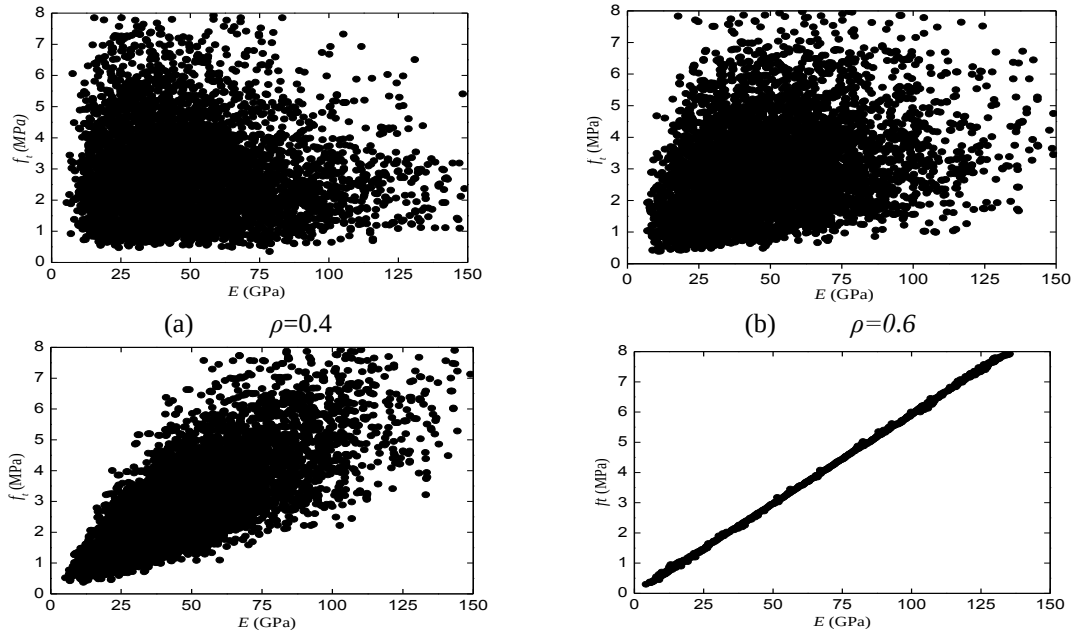

Fig. 8 Probability distribution of E and f_t with different correlation coefficients

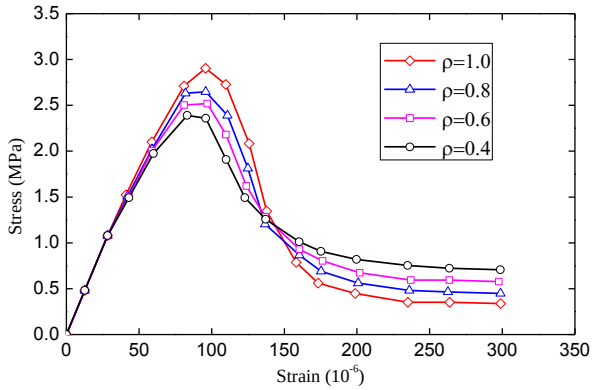

Fig. 9 Comparison of average stress-strain curves with different correlation coefficients

5.2 Influence of the correlation coefficient

In the previous studies, mesh sensitivity, aggregate shape, packing density of aggregate, ITZ's width and mechanical properties were extensively covered (He *et al*. 2011). The correlation coefficient between E and f_t is discussed in the present study. Values of ρ =0.4, 0.6, 0.8, 1.0 are used to inspect the influence on the numerical tensile test. Without loss of generality, each test is verified by 30 numerical analyses. Probability distribution values of E and f_t with different correlation coefficients are shown in Fig. 8. Comparison of average stress-strain curves computed over 30 random simulations of specimens with different correlation coefficients is plotted in Fig. 9.

With strong correlation between E and f_t in the Weibull distribution law, the strength of the specimen is high, and brittle fracture characteristics are more obvious in the failure process, because elements with high elastic modulus have strong strength. Hence, most of the elements achieve the failure criterion at the same time in the same strain. However, with low correlation between E and f_t, elements with high elastic modulus and low strength will first achieve the failure criterion and the load -carrying capacity will decrease so that the stress - strain curve deviates from a straight line. Elements with low elastic modulus and great strength are difficult to damage. Even after peak strength, residual strength still exists. Therefore, strong nonlinear characteristics are presented during the loading process.

5.3 Single-edge notched beam test

Based on the multiphase mesostructure model, a mixed-mode fracture experiment on a single-edge notched (SEN) concrete beam is analyzed by introducing heterogeneities of properties of the three components. The geometry and boundary conditions of the SEN beam are shown in Fig. 10.The length, height, and thickness of the specimen are 675 mm, 150 mm, and 50 mm, respectively. The notch size is 75 mm in depth and 5 mm in width, and is located at the center of the bottom edge of the beam. External loading is imposed at 150mm to the right of the center of the top edge. The concrete beam is discretized using fine meshes (1.67 mm) for the notched area

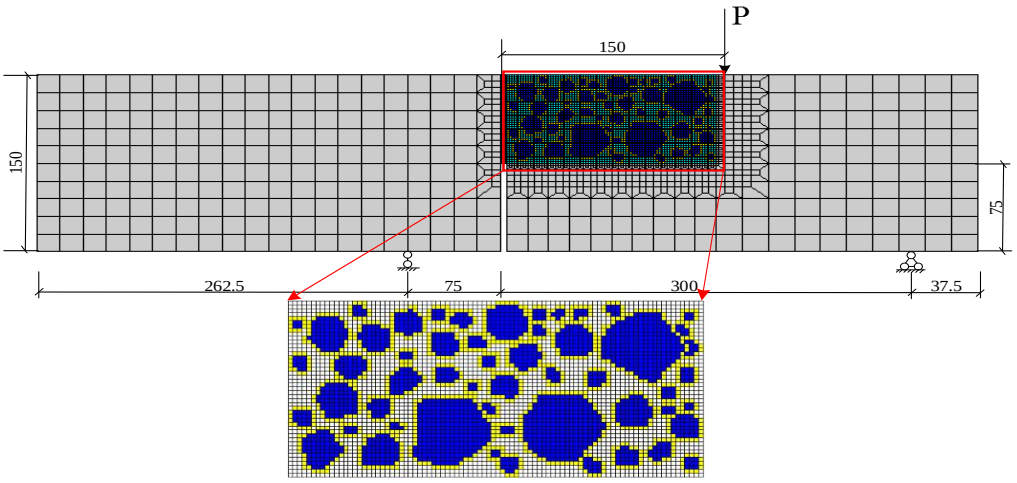

Fig. 10 Geometry and FEM meshes of the single-edge notched beam

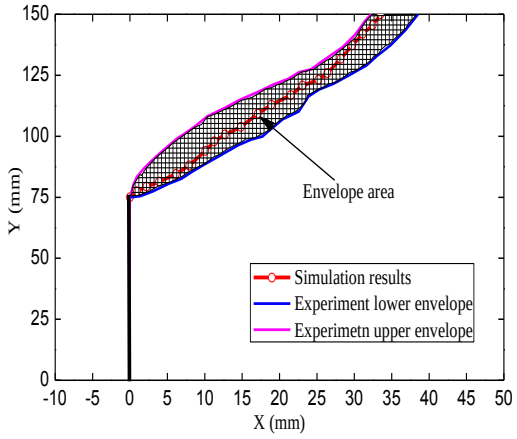

Fig. 11 Crack trajectories of the SEN beam test

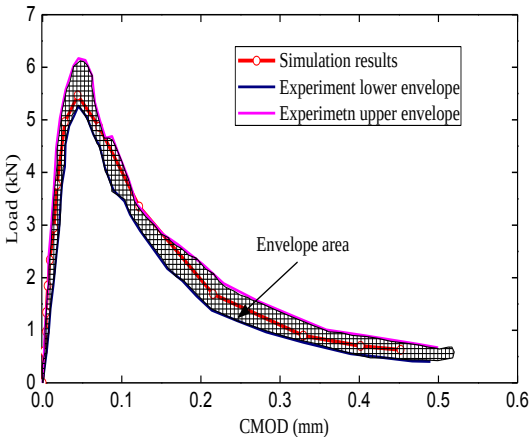

Fig. 12 Load-CMOD curves of the SEN beam test

(150 mm×75 mm) and coarse meshes for the remaining part, as shown in Fig. 10 .There are 4050 elements including aggregates, mortar matrix and interfaces in the notched area. The numerical tests are conducted by applying displacement to the upper point P at a velocity of 1.5×10^{-3} mm each load step in FE calculation, and the corresponding experimental work was performed by Gálvez (Gálvez *et al*. 1998).

Based on the equivalent probabilistic model, mechanical parameters of the three phrases are generated by the above random Weibull distribution, as shown in Table 2. Figure 11 shows a comparison of the crack trajectories between numerical and experimental results. Red and blue lines indicate the crack trajectories of the experimental results by Galvez, while the black line is the main crack path by the presented simulation. The load-CMOD (crack mouth opening displacement) curve obtained in this simulation is shown in Fig. 12 together with the results recorded in the experiments. The crack propagation process by the presented meso-scale model performed successfully and matched well with the experiment. The simulation curves agrees well with the experiment.

6. Modeling temperature cracks of concrete with water-pipe cooling

In this study, the heat-fluid coupling method is introduced to perform the thermal analysis of pipe cooling in concrete, and has proven to be an accurate and applicable simulation method for the analysis of the cooling effect exhibited by water pipes in concrete in previous studies (Liu *et al*. 2012). An investigation into the damage and fracture behavior of the concrete block during water pipe cooling is conducted based on the proposed method. This problem is chosen because it has been extensively studied by other researchers (Zhu1999, Tang Shibin *et al*. 2009). However, all of the previous numerical studies were based on macro-scale modeling, in which concrete was assumed to be homogeneous material. The present studies are focused on the influence of the mechanical parameters on meso-scale random distribution in contrast with macro mechanical parameters obtained through a uniaxial tensile test. In addition, a reasonable temperature difference between concrete and cooling water is studied.

As shown in Fig. 13, a concrete block with a size of 1.5 m × 1.5 m is provided to the mesoscopic

Table 3 Thermal parameters of concrete and cooling water

Prosperity / Material	Heat conductivity (w/m·°C)	Specific heat (J/kg·°C)	Density (kg/m^3)	Coefficient of linear expansion (10^{-6}/°C)
Concrete	2.33	1,050	2,417	8.6
Cooling water	0.161	4,187	1,000	/

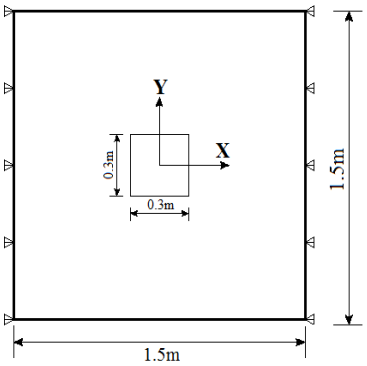

Fig. 13 Geometry of the concrete block

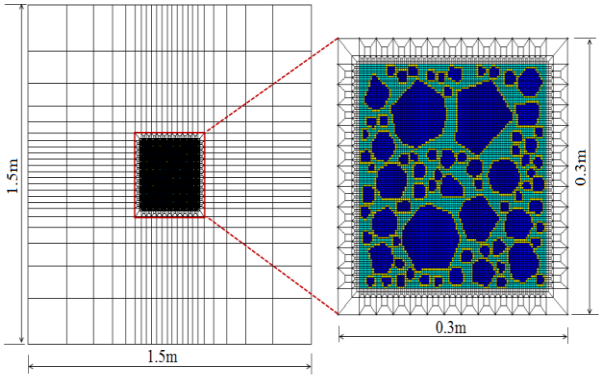

Fig. 14 Finite-element discretization of the concrete block

simulation. The FE model is established for concrete with a water cooling pipe in the middle, which is simulated by the heat-fluid elements. The upper and lower surfaces of the concrete block are set free, while the other two faces are restrained. Only temperature stress is considered. Because of the limit of computational efficiency, a refined mesh of 0.3 m×0.3 m area is used near the cooling pipe where a great temperature gradient is induced by the cooling pipe. The mesh size in this area is sufficiently small for providing the desired accuracy through a posteriori adaptive technique, as shown in Fig. 14. In the calculation of the concrete thermal field, we assume that the three phases of concrete share the same macro thermal parameters. Thermal parameters of concrete and cooling water are shown in Table 3.

6.1 Influence of random distribution of the mechanical parameters

The simulated failure pattern of concrete with macro mechanical parameters used is quite different from that with meso-scale parameters used, which have been covered by other researchers (Hafner *et al*. 2006, Tang *et al*. 2011). In this part, we assume that the initial temperature of the concrete block is 30 °C. The inlet water temperature of the cooling pipe is 10 °C and the water cooling lasts for 20 days. Hence, the initial temperature difference between concrete and the inlet water is 20 °C (Δt = 20 °C). Two comparative cases of numerical experiments are conducted with the same temperature field and FE model. Case 1: only macro homogeneous mechanical parameters are used for all the FEs. Parameters obtained from a uniaxial tensile text with E = 31.3 GPa, f_t = 2.5 MPa, respectively. Case 2: meso-scale mechanical parameters generated by the improved Weibull distribution method of the refined mesh area are used, as shown in Table.2. As a contrast, macro homogeneous mechanical parameters are used for the other coarse FEs.

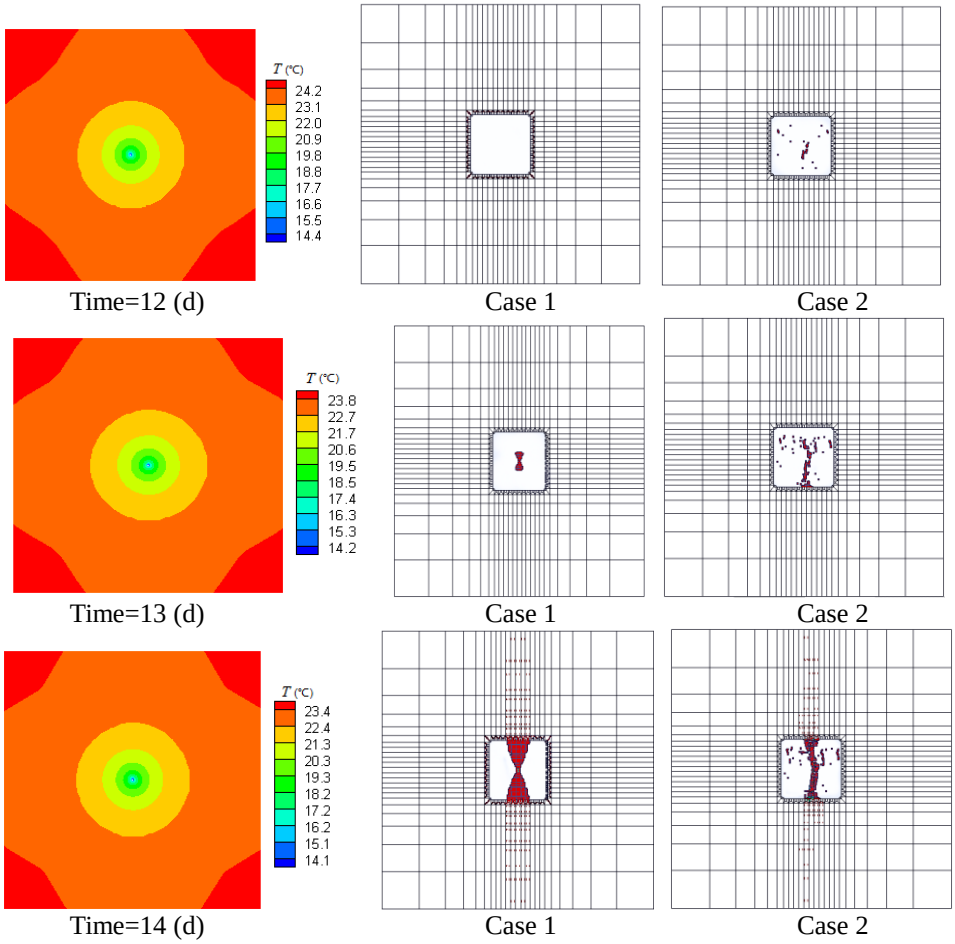

Fig. 15 Temperature-induced failure process of concrete (case1: macro parameters; case 2: meso-scale parameters)

The temperature-induced damage and failure process of the above two comparative cases are shown in Fig. 15 (elements with $D > 0.9$ are shaded red).It can be seen that the closer the concrete gets to the cooling pipe, the lower temperature the concrete is. When water cooling continues to the 12th day, damage has occurred in some weak elements and is mainly concentrated in the refined area near the cooling pipe with meso-scale heterogeneous mechanical parameters. By contrast, there is none damaged element in the concrete with macro homogeneous mechanical parameters. As shown in case 2, before a main crack forms along the cooling pipe, many tiny cracks disperse. Once a main crack forms in concrete near the cooling pipe, it rapidly propagates and concatenates, until the collapse of the entire concrete block. According to the above two cases, the processes take less than a day. The random distribution of mechanical parameters can reflect micro defects existing in the concrete, which are the original cause of damage and cracks. Hence, the heterogeneous mechanical properties have a certain influence on the formation of the initial crack, but have little influence on concrete response under the large temperature tensile stress in a statistical sense.

6.2 Influence of the temperature gradient near the cooling pipe

There is great temperature gradient near cooling pipe, as shown in Fig. 16. Concrete at different distance from the cooling pipe has various degrees of temperature drop during the cooling process. A sharp 10.98 °C temperature decrease occurs at 0.01 m from the cooling pipe, while only a 0.8 °C temperature drop occurs at 0.5 m from the cooling pipe at the beginning of water cooling. There is a fast temperature drop in the early water pipe cooling, because of a large temperature difference between concrete and cooling water, that induces relatively intensive convective heat exchange. As water cooling continues in the concrete, the temperature difference between concrete and cooling water decreases; hence, there is a relatively slow average temperature drop in the concrete.

In this part, the temperature gradient near the cooling water pipe is extensively studied by setting another three different comparative cases. Case 3: only the average temperature drop in Fig. 16 is applied to the concrete block without considering water pipe cooling. Case 4: water pipe cooling is considered, and the inlet temperature of the cooling pipe is 5 °C (This means Δt = 25 °C). Case 5: water-pipe cooling is considered, and the inlet temperature of cooling pipe is 15 °C (Δt = 15 °C). Meso-scale heterogeneous mechanical parameters generated by the improved Weibull distribution method of the refined mesh area are used for these three cases.

Fig. 17 shows the developing process of thermal tensile stress in concrete with different distances from the cooling pipe. It can be seen that the change of thermal tensile stress is closely related to the change of temperature drop inside the concrete. The faster the temperature reduces, the more rapidly the thermal tensile stress rises. By comparison with case 2 and case 3, temperature drop in concrete is extremely uneven. Damage and failure of the concrete occur at different times. When all of the concrete elements suffer from the same temperature load, as shown in case 3, damage and failure seems to occur simultaneously. The larger the initial temperature difference between concrete and cooling water, the sooner the damage and failure occur. Damage occurs on approximately the 5th day after water cooling inside the concrete at 0.01 m from the cooling pipe when Δt = 25 °C. However, the damage occurs on the 6th day and 8th day while Δt=25, 15 °C, respectively.

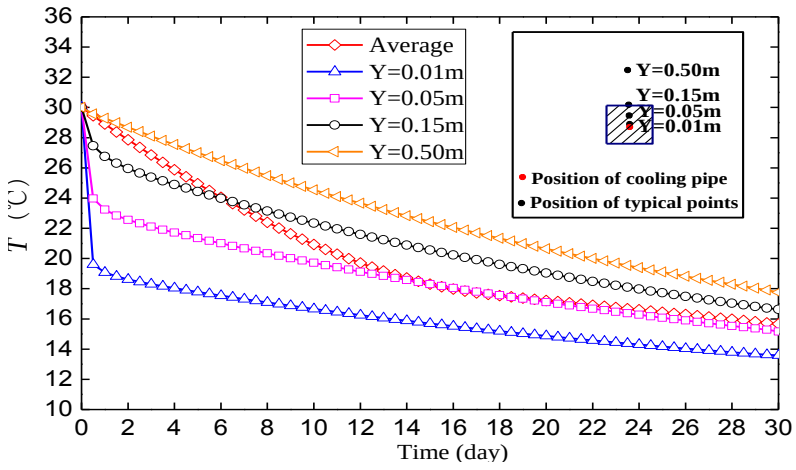

Fig. 16 Temperature drop in concrete with different distances from the cooling pipe

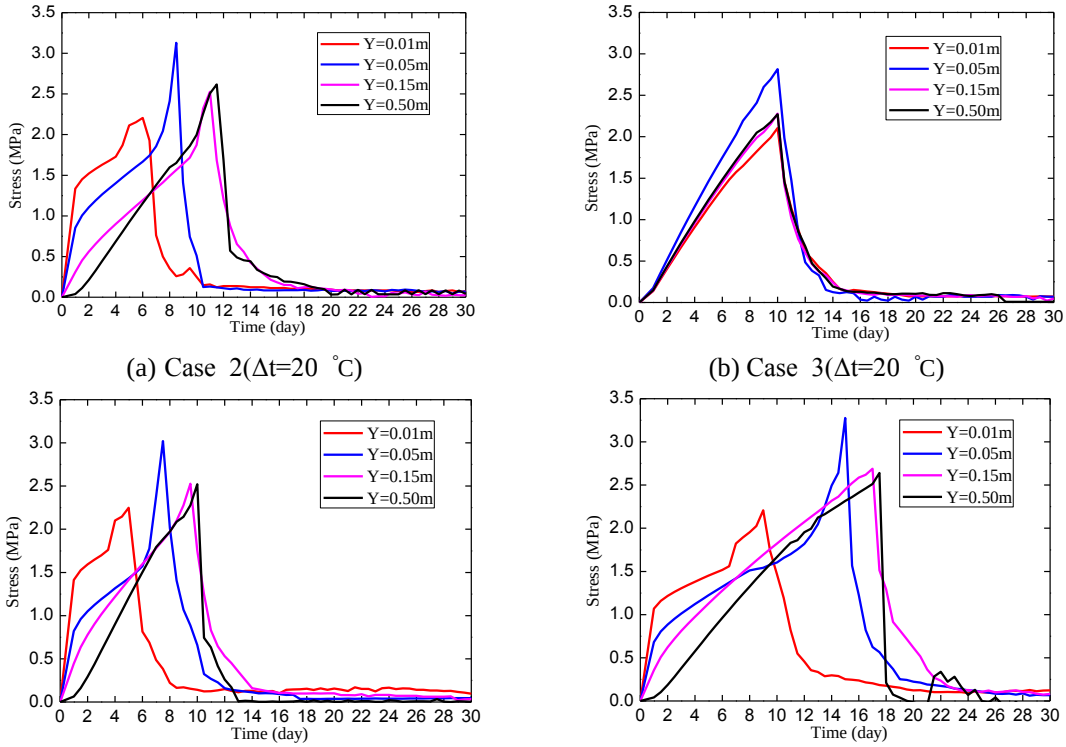

(a) Case 2(Δt=20 ˚C) (b) Case 3(Δt=20 ˚C)

(c) Case 4(Δt=25 ˚C) (d) Case 5(Δt=15 ˚C)

Fig. 17 Thermal tensile stress in concrete with different distance from the cooling pipe

6.3 Results and discussion

Thermal tensile stress in concrete induced by cooling water is mainly caused by two factors: one is the average overall temperature drop in the concrete block; the other is the temperature gradient near the cooling pipe because of the temperature difference between concrete and cooling water. According to the above numerical experiment, we assume that a macro crack form when the length of interconnected damaged elements is greater than 0.1 m. Numerical experiments with meso-scale heterogeneous parameters can fully reflect the weak structure of concrete in the analysis. By contrast, numerical experiments with macro homogeneous mechanical parameters delay the crack appearance time and underestimate risk. In addition, water pipe cooling will lead to uneven temperature distribution. During the concrete's cooling process, the temperature gradient near the cooling pipes is obviously greater, which makes crack more likely to initiate in the concrete near the cooling pipe. The temperature gradient near the cooling pipe should be strictly limited, and for mass concrete in hydraulic engineering, the temperature drop in concrete caused by artificial water pipe cooling is usually 8-10 ˚C; then a reasonable temperature difference between concrete and inlet water temperature is 15-20 ˚C.

Under the same initial and boundary conditions, concrete temperature cracks are mainly affected by heterogeneity of the material, uneven temperature distribution, and overall average temperature drop. The heterogeneity of concrete causes the existence of internal weak parts of

concrete; the overall average temperature drop in concrete is a direct reason for tensile stress by shrinkage; the uneven temperature generates the heterogeneous distribution of temperature stress in time and space, which may also cause stress concentration. The combination of the above three effects is the most unfavorable factor that induces cracks in concrete.

6. Conclusions

A meso-scale model for conventional concrete as a composite with three components of materials, that is, aggregates, mortar matrix and ITZs, is utilized to simulate the failure behavior of concrete, especially temperature-induced cracks in concrete with water pipe cooling. Based on the work presented here, the following conclusions can be drawn:

- An equivalent approach for studying heterogeneity of concrete by introducing the Weibull probabilistic distribution for describing heterogeneities of mechanical and statistical properties of concrete is presented. The three-phase composite of concrete is divided on meso-scale, and the mechanical parameters are selected according to statistical method. Through a series of uniaxial tensile tests, crack initiation, propagation and coalescence are directly exhibited.
- The correlation coefficient ρ between elastic modulus and tensile strength is introduced to improve the Weibull probabilistic distribution. Through a series of uniaxial tensile tests, the influence of the correlation coefficient ρ on failure response of concrete is studied. Additionally, with a larger value of ρ, a comparatively larger tensile strength of the samples, and the brittle characteristic of concrete is more obvious during the failure process. The simulation results of the SEN beam test are in satisfactory agreement with the experimental results and the crack propagation process by the presented meso-scale model is performed successfully and matches well with the experiment.
- The results from a meso-scale numerical investigation into the temperature cracks of concrete with pipe cooling demonstrate that the heterogeneity of concrete material and large temperature gradients near the cooling pipe may have a significant influence on the damage and failure response of concrete. The effect of concrete heterogeneity is clearly shown by the mobilization of distributed temperature-induced damage elements. In addition, the meso-scale random approach predicts more reasonable appearance time and distribution of temperature-induced cracks in concrete with pipe cooling compared to the conventional macro model.

The present study focuses on disclosing the formation mechanism of thermal cracking in concrete induced by temperature drop and temperature gradient near water-cooling pipe through a mesoscopic damage approach. However, it should be emphasized that the cracking of concrete is affected by complicated factors, such as moisture change, creep and autogenous shrinkage, which are not included in this research work. The authors are currently working on another paper in which experiments and consequent influence factors of cracking are intended for further validating the results by the proposed approach.

Acknowledgments

This research investigation was supported by the National Basic Research Program (973 Program) under Grant No. 2013CB035901 and the National Natural Science Foundation of China under Grant NO. 50909078.

References

Amin, M.N., Kim, J.S., Lee, Y. and Kin, J.K. (2009), "Simulation of the thermal stress in mass concrete using a thermal stress measuring device", *Cement Concrete Res*., **39**(3), 154-164.

Wittmann, F.H., Roelfstra P.E. and Sadouki H. (1985), "Simulation and analysis of composite structures", *Mater*. *Sci*. *Eng*., **68**(2), 239-248.

Yaşar, Ergül, Yasin Erdoğan, and Alaettin Kılıç, (2004), "Effect of limestone aggregate type and water–cement ratio on concrete strength", *Mater*. *letters*, **58**(5), 772-777.

Elices, M. and Rocco, C.G. (2008), "Effect of aggregate size on the fracture and mechanical properties of a simple concrete", *Eng*. *Fract*. *Mech*., **75**(13), 3839-3851.

Rocco, C.G. and Elices, M. (2009) "Effect of aggregate shape on the mechanical properties of a simple concrete", *Eng*. *Fract*. *Mech*., **76**(2), 286-298.

He, H., Stroeven, P., Stroeven, M. and Sluys, L.J. (2011), "Influence of particle packing on fracture properties of concrete", *Comput*. *Concr*., **8**(6), 677-692.

Yan, D., and Lin, G., (2006), "Dynamic properties of concrete in direct tension", *Cement Concrete Res*., **36**(7), 1371-1378.

Almusallam, A.A., Beshr, H., Maslehuddin, M. and Al-Amoudi, O.S. (2004), "Effect of silica fume on the mechanical properties of low quality coarse aggregate concrete", *Cement Concrete Compos*., **26**(7), 891-900.

Tang, X.W., Zhou, Y., Zhang, C.H. and Shi, J. (2011), "Study on the heterogeneity of concrete and its failure behavior using the equivalent probabilistic model", *J. Mater. Civil Eng.*, **23**(4), 402-413.

Peerlings, R.H.J. (1999), "Enhaced damage modelling for fracture and fatigue: Proefschrift", Technische Universiteit Eindhoven.

Jirásek, M. and Marfia, S. (2005), "Non-local damage model based on displacement averaging", *Int. J. Numer. Method. Eng.*, **63**(1), 77-102.

Wells, G.N. and Sluys, L.J. (2001), "A new method for modelling cohesive cracks using finite elements", *Int. J. Numer. Method. Eng.*, **50**(12), 2667-2682.

Wanne, T.S and Young, R.P. (2008), "Bonded-particle modeling of thermally fractured granite", *Int. J. Rock Mech. Min. Sci*., **45**(5), 789-799.

Azevedo, N.M., de Lemos, J.V. and de Almeida J.R. (2010), "A discrete particle model for reinforced concrete fracture analysis", *Struct. Eng. Mech.*, **36**(3), 343-361.

Grassl, P., and Jirásek, M., (2010), "Meso-scale approach to modelling the fracture process zone of concrete subjected to uniaxial tension", *Int. J. Solids Struct*., **47**(7), 957-968.

Qian, Z., Ye, G., Schlangen, E. and Van Breugel, K. (2011), "3D lattice fracture model: application to cement paste at micro scale", *Key Eng. Mater*., **452**, 65-68.

Tang, C.A. and Zhu, W.C. (2003), *Concrete Damage and Fracture Numerical Simulate*, Science Press, Beijing, China.

Zhou, X.Q. and Hao, H. (2008), "Mesoscale modelling of concrete tensile failure mechanism at high strain rates", *Comput. Struct*., **86**(21), 2013-2026.

Walraven, J. (1981), "Theory and experiments on the mechanical behavior of cracks in plain and reinforced concrete subjected to shear loading", *Heron*, **26**(1).

Wang, Z.M., Kwan, A.K.H. and Chan, H.C. (1999), "Mesoscopic study of concrete I: generation of random aggregate structure and finite element mesh", *Comput. Struct*., **70**(5), 533-544.

Van Mier, J.G.M. and Shi, C. (2002), "Stability issues in uniaxial tensile tests on brittle disordered materials", *Int. J. Solids Struct*., **39**(13), 3359-3372.

Bazant, Z.P. and Oh, B H. (1983), "Crack band theory for fracture of concrete", *Mater. Struct*., **16**(93), 155-177.

Brekelmans, W.A.M. and De Vree, J.H.P. (1995), "Reduction of mesh sensitivity in continuum damage mechanics", *Acta Mech.*, **110**(1-4), 49-56.

Tang, X.W., Zhang, C.H. and Shi, J.J. (2008), "A multiphase mesostructure mechanics approach to the study

of the fracture-damage behavior of concrete", *Sci. China Series E: Tech. Sci.*, **51**(2), 8-24.
Gálvez, J.C., Elices, M., Guinea, G.V. and Planas, J. (1998), "Mixed mode fracture of concrete under proportional and nonproportional loading", *Int. J. Fract.*, **94**(3), 267-284.
Zhu, B.F. (2013), "Thermal stresses and temperature control of mass concrete", *China Electric Power Press*, Beijing, China, 67-70.
Tang S.B. and Tang, C.A. (2009), "Numerical approach on the thermo-mechanical coupling of brittle material", *Chinese J. Comput. Mech.*, **26**(2), 172-179.
Hafner, Stefan, Stefan Eckardt, Torsten Luther, Carsten Konke, (2006), "Mesoscale modeling of concrete: Geometry and numeric", *Comput. Struct.*, **84**(7), 450-461.

CC